

High Quality Quantum-well Intermixing for InP-based Membrane Photonic Integration on Si

Jieun Lee¹, Kyohei Doi¹, Takuo Hiratani¹, Daisuke Inoue¹,
Tomohiro Amemiya², Nobuhiko Nishiyama¹, and Shigehisa Arai^{1,2}

¹Department of Electrical and Electronic Engineering, ²Quantum Nanoelectronics Research Center
Tokyo Institute of Technology, Meguro-ku, Tokyo 152-8552, Japan

Email address: lee.j.aj@m.titech.ac.jp

Short-Abstract—To realize membrane photonic integrated circuits, a novel quantum-well-intermixing (QWI) process using dual SiO₂ films (O₂-sputtered layer for enhancement of QWI and plasma-deposited layer for surface protection) was investigated. By optimization of the protection layer thickness, a large bandgap wavelength shift difference of 95 nm (57 meV) as well as good photoluminescence (PL) properties (no degradations in the PL spectral width and the intensity) was obtained. Moreover, the transient region length was estimated to be less than 3 μm which is the resolution limit of our PL measurement setup.

I. INTRODUCTION

To realize the optical interconnections on Si-LSIs, we have proposed the concept of the membrane photonic integrated circuit (PIC) [1] as shown Fig. 1. As its components, we have demonstrated membrane lasers [2], photo-detectors [3] and InP-based waveguides [4]. As a photonic integration method of active and passive devices, quantum-well-intermixing (QWI) is expected to be versatile technique by increasing in the bandgap and changing in the refractive-index selectively, with only single epitaxial growth step [5]. Several intermixing techniques have been reported; impurity induced disordering (IID) [6], photo absorption-induced disordering (PAID) [7], and impurity-free vacancy-enhanced disordering (IFVD) [8] in multiple applications.

In this study, we employ the IFVD intermixing method, which relies on creating vacancies in the III-V compound semiconductor during annealing process using dual SiO₂ films for the IFVD intermixing and protection of the surface of non-intermixing region. In regard to the bandgap wavelength shift, the thickness of SiO₂ protection layer is considered as the key parameter for large bandgap wavelength shift between the active and the passive regions.

II. QWI PROCESS

The process flow of our QWI technique is shown in Fig. 2. The initial wafer consists of strain-compensated GaInAsP QWs which include five 6-nm-thick and six 10-nm-thick barriers (90 nm in total) sandwiched by 15-nm-thick GaInAsP ($\lambda_g = 1.22 \mu\text{m}$) layers on a 50-nm-thick InP, 50-nm-thick Be-doped contact layer and double etch-stop layers (InP/GaInAs) grown on (100)-oriented InP substrate by molecular beam epitaxy (MBE). Above the core layer, a 10-nm-thick InP cap was followed by 10-nm-thick GaInAs promotion layers which is designed to promote the intermixing [9] and to cover semiconductor surface during the heating process.

The QWI process was started with the removal of InP cap layer followed by a deposition of 300-nm-thick poor quality

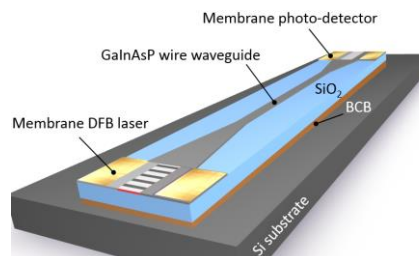


Fig. 1 Schematic representation of membrane photonic integrated circuits.

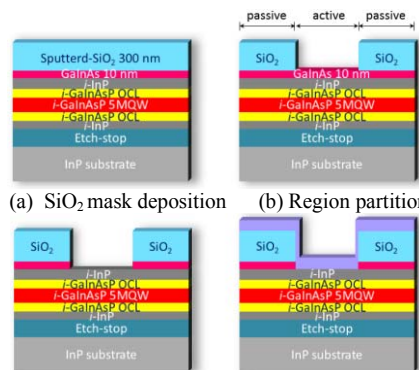


Fig. 2 Quantum-well intermixing process with dual SiO₂ film.

SiO₂ mask, which was for the seeds of vacancies, on the wafer by O₂-sputtering (5 sccm) with a pressure of 1.0×10^{-5} Torr at room temperature [Fig. 2(a)]. Then the wafer was partitioned by photolithography into the active (less wavelength shift is required) and the passive (large wavelength shift is required) regions. After a development of the photoresist, the sputtered SiO₂ mask and the GaInAsP promotion layer on the active region were removed with a wet etching process to suppress bandgap wavelength shift [Fig. 2(b-c)]. Then to protect semiconductor surface during the annealing process, high quality SiO₂ protection layer was deposited on the entire region by plasma-enhanced chemical-vapor deposition (PECVD) [Fig. 2(d)]. Finally, the rapid thermal anneal (RTA) was pursued at 750°C for 180 seconds in nitrogen atmosphere for creating vacancies in the III-V semiconductor. When the dielectric mask formed on III-V wafer is heated in the RTA process, Gallium atoms migrated into the SiO₂ mask layer create group III vacancies and inter-diffused through the quantum-well, then results in QWI.

III. QWI CHARACTERIZATION

Figure 3 shows the PL peak wavelength as a function of the thickness of the PECVD-SiO₂ protection layer tuned to 20, 50,

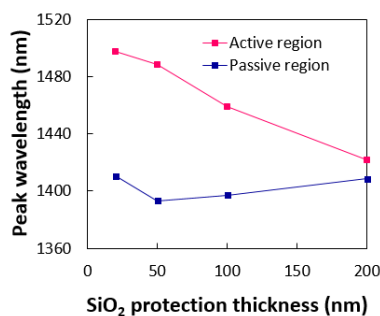


Fig. 3 Peak wavelength as a function of SiO₂ protection layer thickness.

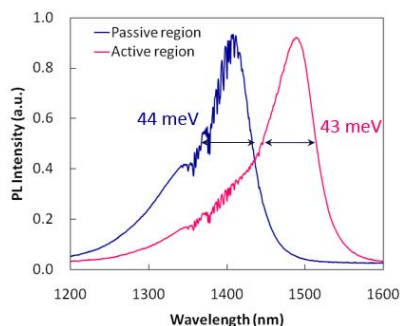


Fig. 4 Photoluminescence spectra of protection layer 50 nm.

100, and 200 nm where the pump beam of $\lambda_p = 640$ nm (power: 21 mW) was used. When the protection layer thickness was 50 nm, the PL peak wavelength shift was 132 nm (77 meV) and the full width at half maximum (FWHM) was 44 meV in the passive region. On the other hand, the PL peak shift was 37 nm (20 meV) and the FWHM was 43 meV in the active region, hence the bandgap wavelength shift difference of 95 nm (57 meV) was obtained. This difference was much larger than that with 200-nm-thick protection layer [10]. Since the low density of point defects was generated on the PECVD-SiO₂ protection layer as well, the blue-shift on the active region with thick protection layer increased due to the large point defects concentration.

Additionally, the PL spectra of 50-nm-thick protection layer are shown in Fig. 4, the intensity ratio of the active to the passive regions was 0.97, which was better than 0.73 for the case of 20-nm-thick protection layer, because 50-nm-thick protection layer was not excessively thin and enough to prevent heat damage of wafer during the RTA. Please note the ripples shown on the PL spectra around wavelength 1380nm were just artificial effect due to water absorption in the air during the measurement.

To confirm the transient region length at the boundary between the active and the passive regions, PL mapping was carried out with $3 \times 3 \mu\text{m}^2$ resolution [Fig. 5(a)]. In order to prevent optical absorption loss in the waveguide which is contiguous to active device such as laser and photo-detector, it is desirable to form sharp transient region. Figure 5 (b) indicates the peak wavelength on the boundary between active (1488 nm) and passive region (1393 nm). The PL spectrum showed dual peak structure and no peaks between them, this means that the transient region length is much smaller than the resolution (less than 3 μm).

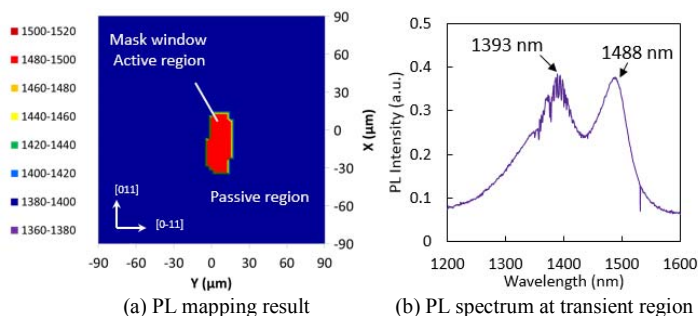


Fig. 5 PL measurement results of peak wavelength in 50 nm protection.

IV. CONCLUSION

In conclusion, we improved QWI process using dual SiO₂ films for membrane photonic integration and obtained 95 nm bandgap wavelength shift difference with transient region length of less than 3 μm (resolution limit) by optimizing SiO₂ protection layer thickness. At the same time, PL intensity ratio of active to passive region was obtained to be 0.97 resulted from proper thickness to avoid the damage during RTA process.

ACKNOWLEDGEMENT

This work was supported by JSPS KAKENHI (Grant numbers 24246061, 2570926, 21226010, 25420321, and 13J08092), the Council for Science and Technology Policy (CSTP) under the FIRST program.

REFERENCES

- [1] S. Arai, N. Nishiyama, T. Maruyama, and T. Okumura, "GaInAsP/InP membrane lasers for optical interconnects," *IEEE J. Sel. Top. Quantum Electron.*, vol. 17, no. 5, pp. 1381-1389, Oct. 2011.
- [2] K. Doi et al., "Room-temperature continuous-wave operation of lateral current injection membrane laser," *Proc. Int. Conf. Indium Phosphide and Related Materials*, WeD2-3, May 2013.
- [3] Y. Yamahara et al., "Characterization of GaInAsP lateral junction waveguide type membrane photodiode," the Institute of Electronics, Information and Communication Engineer, C-4-15, Sep. 2012.
- [4] J. Lee et al., "Low-loss GaInAsP wire waveguide on Si substrate with benzocyclobutene adhesive wafer bonding for membrane photonic circuits," *Jpn. J. Appl. Phys.* vol. 51, no. 4, pp. 042201-1-042201-5, Apr. 2012.
- [5] J. W. Raring et al., "Demonstration of widely tunable single-chip 10-Gb/s laser-modulators using multiple-bandgap InGaAsP quantum-well intermixing," *IEEE Photon. Technol. Lett.*, vol. 16, no. 7, pp. 1613-1615, July 2004.
- [6] D. Deppe and N. Holonyak, Jr., "Atom diffusion and impurity-induced layer disordering in quantum well III-V semiconductor heterostructures," *J. Appl. Phys.* vol. 64, no. 12, pp. 93-113, Dec. 1988.
- [7] B. Qui, A. Bryce, R. De La Rue, and J. Marsh, "Monolithic integration in InGaAs-InGaAsP multiquantum-well structure using laser processing," *IEEE Photon. Technol. Lett.*, vol. 10, no. 6, pp. 769-771, June 1988.
- [8] S. K. Si, D.H. Yeo, K. H. Yoon, and S. J. Kim, "Area selectivity of InGaAsP-InP multiquantum-well intermixing by impurity-free vacancy diffusion," *IEEE J. Sel. Topics Quantum Electron.*, vol. 4, no. 4, pp. 619-623, June/Aug. 1988.
- [9] H. S. Kim et al., "Quantum well intermixing of In_{1-x}Ga_xAs/InP and In_{1-x}Ga_xAs/In_{1-x}Ga_xAs_{1-y}P_y multiple-quantum-well structures by using the impurity-free vacancy diffusion technique," *Semicond. Sci. Technol.*, vol. 15, no. 10, pp. 1005-1009, Jul. 2000.
- [10] J. Lee et al., "Bandgap wavelength shift in quantum well intermixing using different SiO₂ masks for photonic integration," *Proc. Int. Conf. Indium Phosphide and related materials* P3-19, May 2013.